



Self-equalizing photodiodes, a hybrid electro-optical approach to tackle bandwidth limitation in high-speed signaling

BEHROOZ ABIRI,^{1,*} FIROOZ AFLATOUNI,^{1,2} AND ALI HAJIMIRI¹

¹Department of Electrical Engineering, California Institute of Technology, Pasadena, CA 91125, USA

²Department of Electrical and Systems Engineering, University of Pennsylvania, 200 South 33rd St., Philadelphia, PA 19104, USA

*babiri@caltech.edu

Abstract: In this paper we provide the design details of self-equalizing photodetectors which enable higher data rate transmission by improving the overall bandwidth of the bandwidth limited transmission link, through a hybrid electro-optical solution. Two different self-equalizing photodiodes, one having fixed equalization and the other being programmable are presented as proof of concept.

© 2017 Optical Society of America

OCIS codes: (130.0130) Integrated optics; (250.5300) Photonic integrated circuits; (040.5160) Photodetectors; (130.3120) Integrated optics devices; (250.3140) Integrated optoelectronic circuits; (250.4745) Optical processing devices.

References and links

1. T. S. Rappaport, *Wireless communications: principles and practice*, Vol. 2, (Prentice Hall PTR, 1996).
2. K. Azadet, E. F. Haratsch, H. Kim, F. Saibi, J. H. Saunders, M. Shaffer, L. Song, and M. L. Yu, "Equalization and FEC techniques for optical transceivers," *IEEE J. Solid-State Circuits* **37**(3), 317–327 (2002).
3. S. Gondi and B. Razavi, "Equalization and Clock and Data Recovery Techniques for 10-Gb/s CMOS Serial-Link Receivers," *IEEE J. Solid-State Circuits* **42**(9), 1999–2011 (2007).
4. A. H. Gnauck, C. R. Doerr, P. J. Winzer, and T. Kawanishi, "Optical Equalization of 42.7-Gbaud Bandlimited RZ-DQPSK Signals," *IEEE Photonics Technol. Lett.* **19**(19), 1442–1444 (2007).
5. C. R. Doerr, S. Chandrasekhar, P. J. Winzer, A. R. Chraplyvy, A. H. Gnauck, L. W. Stulz, R. Pafchek, and E. Burrows, "Simple multichannel optical equalizer mitigating intersymbol interference for 40-Gb/s nonreturn-to-zero signals," *J. Lightwave Technol.* **22**(1), 249–256 (2004).
6. C. R. Doerr, A. H. Gnauck, L. W. Stulz, and D. M. Gill, "Using an optical equalizer to transmit a 43-Gb/s signal with an 8-GHz bandwidth modulator," *IEEE Photonics Technol. Lett.* **15**(11), 1624–1626 (2003).
7. H. Yun, W. Shi, Y. Wang, L. Chrostowski, and N. A. Jaeger, "2×2 adiabatic 3-dB coupler on silicon-on-insulator rib waveguides," *Proc. SPIE* **8915**, 89150V (2013).
8. S. Chen, Y. Shi, S. He, and D. Dai, "Low-loss and broadband 2×2 silicon thermo-optic Mach-Zehnder switch with bent directional couplers," *Opt. Lett.* **41**(4), 836–839 (2016).
9. B. Abiri, F. Aflatouni, and A. Hajimiri, "A self-equalizing photo detector," in *IEEE Photonics Conference*, San Diego, CA (2014), pp. 196–197.
10. B. Abiri, A. Zhou, F. Aflatouni, and A. Hajimiri, "An Adjustable Self-Equalizing Photo Detector," in *Optical Fiber Communication Conference, OSA Technical Digest* (2015), paper W3A.3.
11. M. Streshinsky, R. Ding, Y. Liu, A. Novack, C. Galland, A. J. Lim, P. G. Lo, T. Baehr-Jones, and M. Hochberg, "The Road to Affordable, Large-Scale Silicon Photonics," *Opt. Photonics News* **24**(9), 32–39 (2013).
12. A. Novack, M. Gould, Y. Yang, Z. Xuan, M. Streshinsky, Y. Liu, G. Capellini, A. E. Lim, G. Q. Lo, T. Baehr-Jones, and M. Hochberg, "Germanium photodetector with 60 GHz bandwidth using inductive gain peaking," *Opt. Express* **21**(23), 28387–28393 (2013).
13. T. T. Aalto, M. Kapulainen, S. Yliniemi, P. Heimala, and M. J. Leppihalme, "Fast thermo-optical switch based on SOI waveguides," *Proc. SPIE* **4987**, 149 (2003).
14. H. Chen, P. Verheyen, P. De Heyn, G. Lepage, J. De Coster, S. Balakrishnan, P. Absil, W. Yao, L. Shen, G. Roelkens, and J. Van Campenhout, "−1 V bias 67 GHz bandwidth Si-contacted germanium waveguide p-i-n photodetector for optical links at 56 Gbps and beyond," *Opt. Express* **24**(5), 4622–4631 (2016).

1. Introduction

One of the greatest challenges in increasing optical data transmission rates is the inherent bandwidth limitations of electrical and electro-optical components of the communication link. In a bandwidth limited data transmission link, the high frequency components of the

transmitted data generally get attenuated more than the lower frequency components of the spectrum. The result of this bandwidth limitation is often closed eye diagrams on the receiver side where it will be more challenging for the receiver circuitry to recover the data.

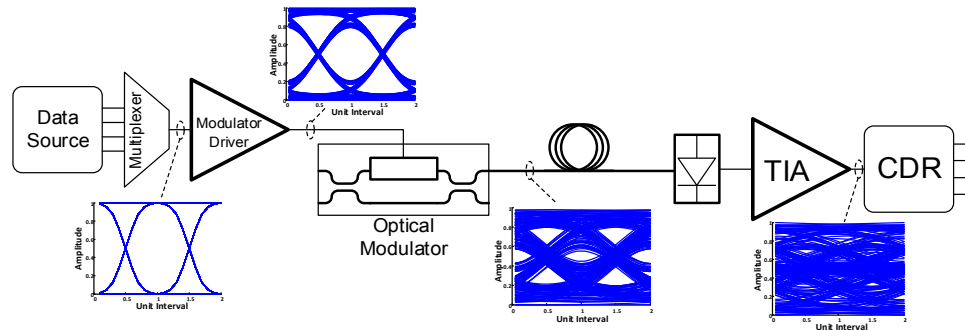


Fig. 1. Effect of bandwidth limited electrical and electro-optical components on the transmitted data. A simple threshold based data recovery is not possible after removing the high frequency content of the signal.

The problem of channel bandwidth limitation is well studied [1,2]. In wireline communication technology, where low bandwidth electrical transmission lines are used, bandwidth limited distortion of the signal has been addressed through equalization techniques. These techniques essentially restore the signal by introducing a high-pass filter into the data link. The role of the high pass filter is to balance the ratio of the high frequency components to the low frequency components of the received signal. Since the bandwidth limitation in wireline communication is mainly dominated by the channel and not the electronic circuitry, the equalizers can easily be implemented in the electronic circuitry. In optical links, however, the bandwidth limitation arises from the electronic circuitry and the electro-optical components. In such systems, implementing equalizers in already bandwidth limited electronics is challenging and thus equalizers need to be implemented in the optical domain, which can suffer from its own shortcomings.

In this paper, we present a hybrid electro-optical approach for equalizing the receiver signal in the photodiodes of an optical link. Section 2 provides a brief background on the effects of bandwidth limitation on data transmission and how equalization overcomes these effects. Section 3 explains our proposed hybrid electro-optical approach. Measurement results are presented in section 4, and the paper is concluded in section 5.

2. Background

The data transmitted through bandwidth limited electrical and electro-optical components in an optical link will lose most of its high frequency content. This effectively smoothens the received data waveform. If the bandwidth of the link is much smaller than half of the symbol rate, the received data will be distorted to the extent such that a simple threshold based data estimator will not work (Fig. 1).

By implementing a high pass filter in the transmitter side, receiver side, or both, it is possible to reverse the distortions caused by the band-limited components. In wireline communications, high-pass filters in the transmitter side will increase EMI to adjacent channels, while in WDM systems, it will increase the crosstalk between the channels if not enough guard band is put in place. On the other hand, placing the high pass filter in the receiver side will deteriorate the sensitivity of the receiver. This is because the high pass filter attenuates the lower frequency components of the signal to level the overall frequency response and as a result the overall signal power will be lowered relative to noise. This reduction in overall signal to noise ratio can be somewhat mitigated by placing an amplifier before the equalizer.

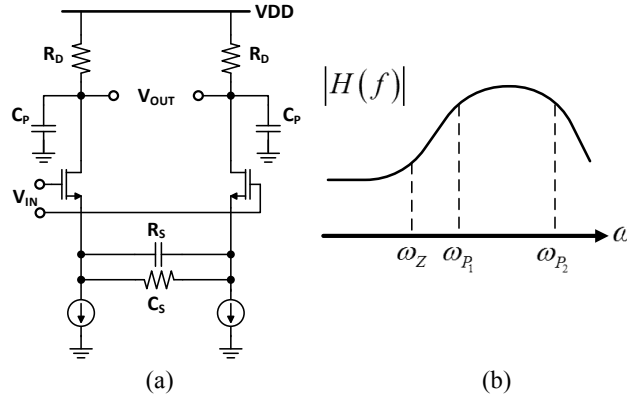


Fig. 2. (a) Example of equalizers implemented in electrical domain [3]. (b) Typical transfer function of electrical equalizers. Due to parasitic capacitances, such equalizers are band-limited.

In an optical data communication link, the receiver equalizer can be placed either in optical or in electrical domain of the receiver. An example of equalizer implemented in the electrical domain is shown in Fig. 2(a) [3], where the high-pass filter is integrated with the amplifier to form an active high-pass filter. The electrical amplifier has a limited bandwidth and as a result the frequency response starts to drop beyond a certain frequency (Fig. 2(b)). In summary, the equalizer implemented in the electrical domain benefits from tunability, flexibility, and the ease of amplification of the signal before equalization, however, such an equalizer is limited by the bandwidth of the technology used.

An optical equalizer, on the other hand, can enjoy the wide bandwidth of the optical system [4-6]. An example of optical equalizer reported in [6] is shown in Fig. 3(a) where an optical filter is formed using Mach-Zehnder Interferometer (MZI) structures. The optical filter produces a sine wave shaped response and by setting the center of the valley of the response to the laser wavelength (carrier frequency) it is possible to equalize the data transmission (Fig. 3(b)). As shown in Fig. 3(c), the equalization is sensitive to deviation of frequency of the laser or drift in the optical filter. As a result, tight temperature control loops are required to assure minimal frequency deviation of the laser and the filter. We will briefly analyze the operation of

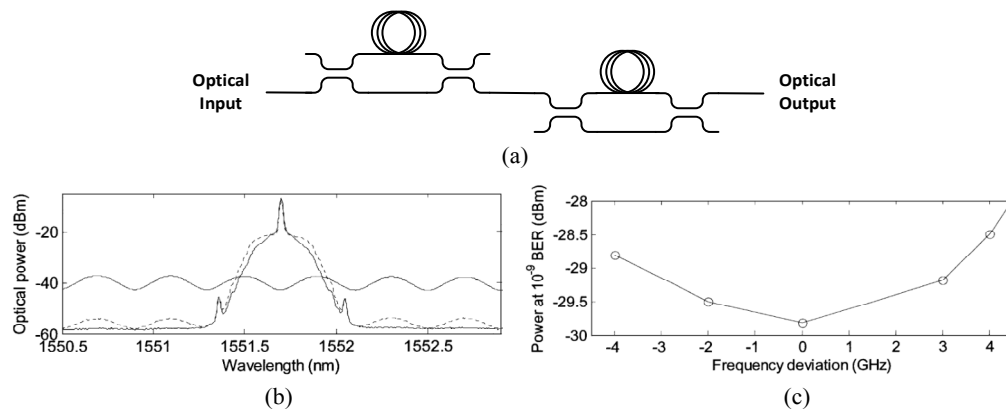


Fig. 3. (a) An example of optical equalizer implementation [6]. (b) Measured optical spectra of the modulated signal without (solid line) and with (dotted line) equalization. The sinusoidal line shows the transmissivity through the equalizer. (c) Equalizer sensitivity vs. laser frequency deviation [6].

an MZI based optical equalizer to explain the source of the sensitivity of the optical equalizer to frequency deviation of the laser.

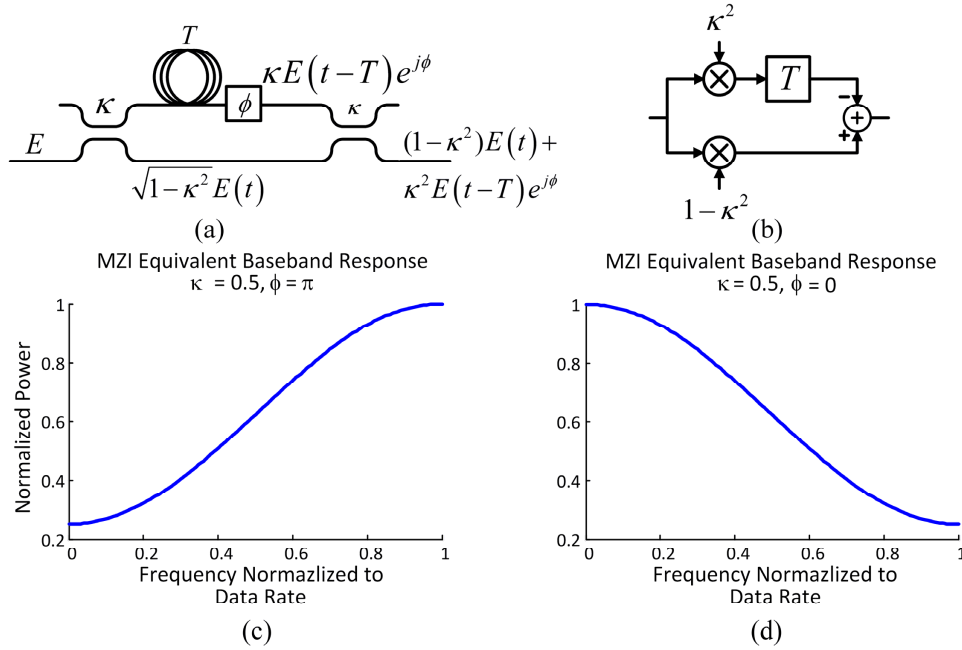


Fig. 4. (a) Example of an FIR optical equalizer implementation. (b) Block diagram of the desired filter. (c) An example of desired response. (d) Undesired response of same implementation due to laser wavelength drift.

The high-pass filter for an optical equalizer can be easily implemented with an MZI structure acting as an FIR filter. Such a filter as shown in Fig. 4(b), equalizes the received signal by subtracting a proportion of delayed version of the input signal from the non-delayed proportion. An optical waveguide can provide the delay, while the subtraction is done in the right hand side coupler of the MZI shown in Fig. 4(a). If the output of the MZI is fed to a photodiode the output current would be:

$$I_{out} = R \left[(1-\kappa^2)^2 P(t) + \kappa^4 P(t-T) + 2\kappa^2 (1-\kappa^2) \sqrt{P(t)P(t-T)} \cos(\phi) \right]$$

where R is the photodiode responsivity, $P(t)$ is the input optical power, κ is the coupling coefficient of the coupler in the MZI, T is the delay of the waveguide, and $\phi = \omega_0 T$ is the phase shift associated with the delay line at laser frequency, ω_0 .

This presents several challenges. First the profile of the response (Fig. 4(b) and 4(c)) cannot be fully controlled, leading to suboptimal results. Second, the frequency response of the equalizer is dependent on ϕ . Two examples of equalizer frequency response are shown in Fig. 4 (c) and (d) for $\phi = \pi$ and $\phi = 0$, respectively. For $\phi = \pi$, the combiner properly subtracts the delayed version of the input from the non-delayed version and hence the equalizer acts as a high-pass filter, as intended. However, if due to frequency drift of the laser, ϕ becomes zero, the combiner adds the two optical signals and as a result, the frequency response of the equalizer becomes a low-pass one. Due to process variation in fabrication and temperature fluctuations, the exact effective index of an optical waveguide and hence the value of ϕ cannot be determined *a priori*, hence control loops are required to assure $\phi = \pi$ for the operating wavelength.

In the following section we describe how to resolve the laser wavelength dependency of the optical equalizer by proposing a hybrid electro-optical approach.

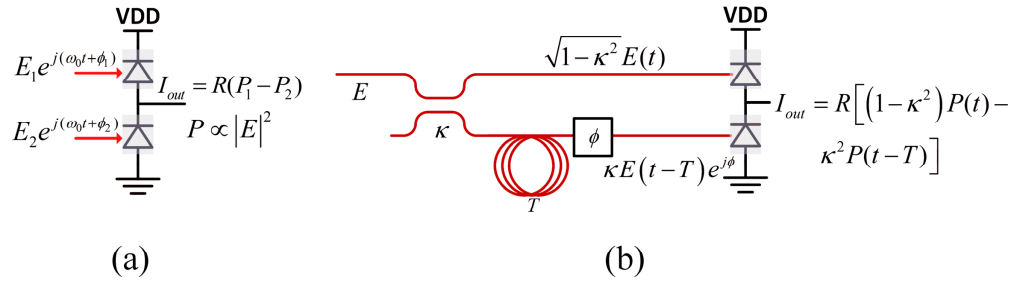


Fig. 5. (a) Optical phase independent subtraction by using photodiodes. (b) A carrier wavelength insensitive hybrid electro-optical equalizer.

3. Design and implementation

As mentioned in the previous section, the root cause of the wavelength dependency of the equalizer is the optical combiner, where subtraction of the delayed signal from non-delayed signal is sensitive to the wavelength drift of the laser. In order to remove this sensitivity, we propose to convert the optical signals to an electrical signal through a photodetector and then perform the subtraction in the electrical current domain. A photodiode produces a photocurrent proportional to its input optical power, irrespective of the input optical phase. Subtraction of the delayed signal from the non-delayed one can be done in current mode by simply connecting the output of photodiodes to the same node such that one sources current while the other sinks it, as shown in Fig. 5(a). By removing the right-hand side combiner of equalizer in Fig. 4(a) and substituting it with a photodiode based subtraction circuit a hybrid electro-optical equalizer is achieved. Hence, the output current of the equalizer shown in Fig. 5(b) can be written as:

$$I_{out} = R[(1 - \kappa^2)P(t) - \kappa^2 P(t - T)]$$

As it can be seen from the equation, the frequency response of the equalizer in this case is not dependent on the carrier laser wavelength. It should be noted that carrier wavelength sensitivity of the equalizer is not completely removed as the coupling factor of the directional coupler, κ , which sets the equalization strength, is still wavelength dependent; however, this dependency is significantly lower than what is achievable with purely optical equalizers. Also there exist approaches that increase the bandwidth of the coupler and reduce the wavelength sensitivity [7,8].

As a proof of concept we developed two different equalizers [9,10] that implement the same concept demonstrated in 5(b) but for higher order equalizers in a silicon-photonics platform provided by IME. The details of the platform is provided in [11]. The system integrates all the equalization functionalities as well as optical to electrical conversion in one chip, hence, it can be viewed as a self-equalizing photodetector (SEPD).

The block diagram of the two tap implemented prototype is shown in Fig. 6(a). The input optical signal is split by a ratio of 23/77 by the first directional coupler. The larger portion of the split enters a photodiode without further added delay while the smaller portion passes through a 50ps delay line before splitting by another directional coupler with split ratio of 34/66. The thru portion of the coupler directly enters the second photodiode while the coupled portion is further delayed by 50ps before opto-electrical conversion. The electrical current produced by the delayed optical signals is subtracted from the current produced by the zero-delay optical signal, resulting in a signal flow diagram shown in Fig. 6(b). The frequency response of the equalizer can be expressed as:

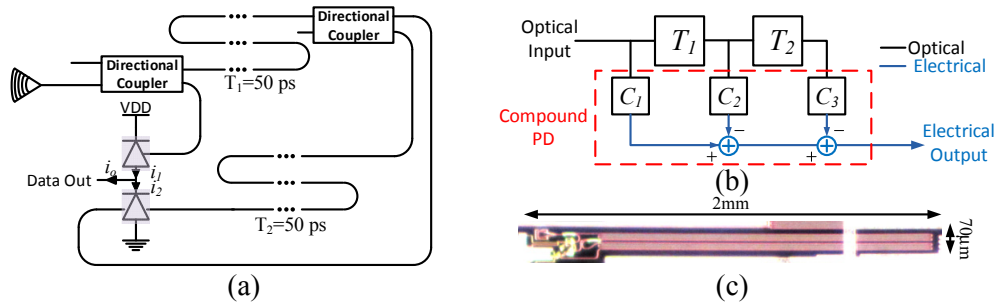


Fig. 6. Implemented 2-tap self-equalizing photodetector. (a) The block diagram. (b) Equivalent signal flow diagram. (c) Die photo of the implemented IC.

$$I_{out} = C_1 - C_2 e^{-j\omega T} - C_3 e^{-2j\omega T}$$

where $C_1 = RP(1 - \kappa_1^2)$, $C_2 = RP\kappa_1^2(1 - \kappa_2^2)$, and $C_3 = RP\kappa_1^2\kappa_2^2$ are set by the coupling coefficients, κ_1 and κ_2 , of first and second directional coupler, respectively.

In order to minimize the number of photodiodes and hence the capacitive loading of the output node, a dual input photodiode (DIPD) is proposed. The structure of a dual input photodiode is shown in Fig. 7(a). The vertical buildup of the diode is similar to the single input work reported in [12]. By adding a second optical input in the opposite direction of the first optical input, it is possible to effectively sum the optical power of the two signals and convert them to electrical current within one photodiode structure, cutting the overall junction capacitance on the summing node by half. The relative phase of the optical signals has no effect on the output current, as the optical signals travel in the opposite directions of each other.

While the SEPD provides a simple solution to improve the bandwidth of communication channel and hence increase the data rate, it does not allow for dynamic bandwidth adjustment. In order to provide a more flexible solution and to be able to adjust the bandwidth enhancement of the equalizer, programmable coupling factors are required. Also, to be able to equalize a more variety of data rates and channels, a larger number of taps with smaller delays must be utilized.

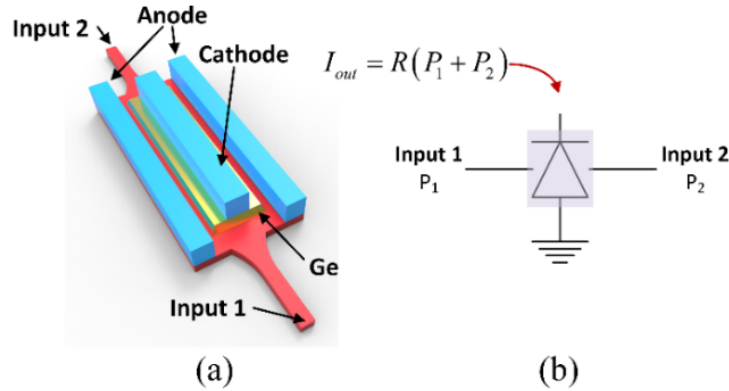


Fig. 7. (a) Dual input photodiode and (b) its symbol. Optical power of two signal is summed and converted to electrical current within one junction.

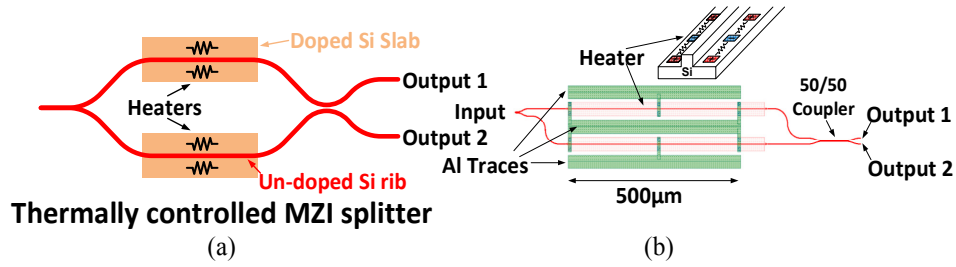


Fig. 8. Dynamic tap coefficient adjustment with a thermally controlled MZI. (a) Schematic diagram of the MZI and (b) the corresponding layout. Heaters are implemented by doping the slab section of the waveguide and passing current through them.

To adjust the frequency response of the equalizer, the tap coefficients of the FIR filter need to be programmable. This can be easily achieved by dynamically controlling the intensity of light incident on each photodiode. A thermally controlled MZI 1x2 optical switch is used to dynamically control the optical power flow [13]. The schematic and layout of the thermally controlled MZI is shown in Fig. 8. The input power is split between the two outputs of the MZI with an adjustable ratio by controlling the amount of the phase shift between the two arms of the MZI. The phase shift is introduced by heating the waveguide in one arm of the MZI and hence changing the refractive index of the silicon waveguide. In order to minimize the amount of electrical power needed for a desired phase shift, the resistive heaters are implemented in the slab section of a strip-loaded waveguide by doping the slab section of the waveguide. This assures that the least thermal resistance of the heaters to the waveguide as thermal conductivity of silicon is almost 100 times that of silicon dioxide. Another method used to reduce the electrical power needed for adjusting split ratio is to place thermal phase shifters on each arm of the MZI. Only one arm of the MZI is heated at any time. This will reduce the maximum required phase shift provided by the phase shifters to 90° compared to 180° needed when only one phase shifter is used and hence reduces the power consumption by a factor of two.

As a demonstration of the concept, we designed a prototype implementing the signal graph flow shown in Fig. 9(b) with $T = 25 ps$. The block diagram of the design is shown in Fig. 9(b). As it can be seen from the signal flow graph, the first two tap coefficients, C_0, C_1 have a fixed sign, while the sign of the other coefficients are selectable. The sign of the coefficient can be set by selecting the direction of the photo current in the output node. If the photocurrent is added to the output node, the sign is positive and if it is subtracted the sign is negative. This can be achieved by placing the photodiodes as shown in Fig. 9(a) and use an optical switch to route the optical signal of the corresponding tap coefficient to either the upper or the lower photodiode. Each tap that has a selectable sign needs an optical splitter. So the optical splitters 4, 6, and 7 in Fig. 9(a) select the sign of the coefficients while the optical splitters 1, 2, 3, and 5 select the tap coefficients. The overall frequency response of the adjustable self-equalizing photodiode (ASEPD) can be hence written as:

$$I_{out} = RP \left[C_0 - C_1 e^{-j\omega T} \pm C_2 e^{-j2\omega T} \pm C_3 e^{-j3\omega T} \pm C_4 e^{-j4\omega T} \right]$$

where R is the responsivity of the photodiodes, P is the input optical power, and C_0 to C_4 are the adjustable tap coefficients.

Processing the light in order to equalize the signal will result in some extra loss which will degrade the SNR of the recovered signal, however, in a bandwidth limited system the BER will suffer mainly from distortion of the received data. Nonetheless, the excess loss from the optical components is as follows. The loss from the directional couplers are very small and in the order of 0.01dB and the loss from the thermal phase shifters are around 0.06dB, so the overall loss of the adjustable phase splitter is around 0.07dB. The delay lines have a loss of

0.32dB/cm. As a result each 25ps delay line has 0.064dB of excess loss. It should be noted that the main tap, C_0 , which carries most of the optical power, does not go through a delay line and the contribution of the loss of the other delay lines depends on the amount of equalization needed from corresponding taps. The main loss in our system comes from the grating coupler which has a loss of 3.5dB.

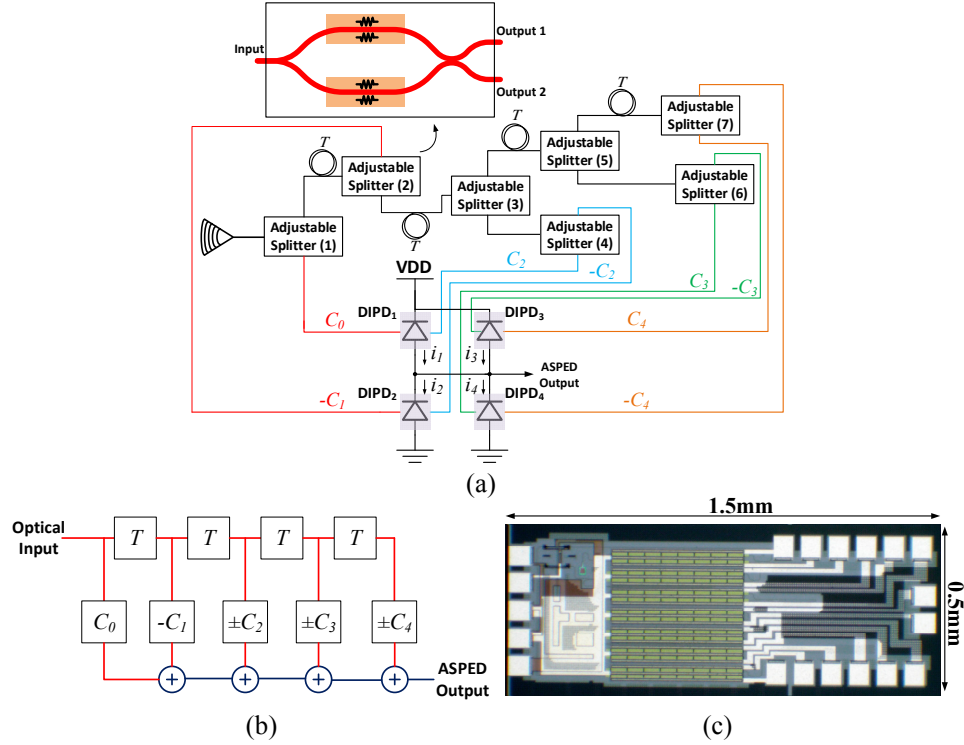


Fig. 9. (a) The block diagram of implemented adjustable self-equalizing PD (ASEPD) and (b) its signal flow diagram, (c) the die photo of the ASEPD

In this design we used DIPD to keep the capacitance loading of the output node low. However, due to increased number of taps, the number of photodiodes attached to the output node is doubled compared to the previous implementation. In order to reduce the drop in bandwidth due to capacitive loading, photodiodes corresponding to higher tap coefficients are designed to be smaller than the photodiode of tap C_0 . While reducing the length of the photodiodes slightly reduces the responsivity, the sensitivity of the receiver is not reduced noticeably given the smaller photocurrent needed for the higher tap coefficients. Based on recent advances in Ge photodiodes implemented on silicon photonics platform, the bandwidth of the photodiode is mainly dictated by the transit time of the carriers and as a result the junction capacitance of the photodiode is no longer a limiting factor in the bandwidth [14]. The reason that the transit time cannot be reduced significantly in waveguide photodiodes is that the optical mode in the photodiode has to have reasonable overlap with the photodiode's depletion or intrinsic region; otherwise, the responsivity of the photodiode will suffer due to the optical loss caused by the metal contacts or highly doped regions of the junction. By utilizing such photodiodes, there would be very small bandwidth penalty due to extra capacitive loading at the output node because of multiple photodiodes. This means that SEPDP concept can be utilized to enhance the bandwidth limitation of transit-time limited photodiodes as well as bandwidth limitation due to other components in the transceiver link as long as the bandwidth of the optical link is not limited by the capacitance of the photodiodes.

The bandwidth limitation of the photodiodes that we used in IME process were mainly dominated by the large series resistance of the photodiode (i.e. the contact resistance). The detrimental effect of increasing junction capacitance due to multiple photodiode is to some extent offset by the reduction of the photodiode resistance. In our ASEPD prototype example, the total junction capacitance at the output is estimated to be 100fF [12] which we estimate to provide 21GHz of bandwidth (including the 50 ohm impedance of network analyzer), sufficient for the 25Gbps target operation.

4. Measurement results

To demonstrate the equalization capability of the two-tap SEPD, its performance was compared against a 35GHz photodiode in a 12.5Gbps data link. In Fig. 10(b) we can see that the electro-optical frequency response of the channel is improved by using the proposed SEPD. The channel frequency response shows a very low 3dB bandwidth of 1.5GHz when a 35GHz photodiode is used. The SEPD is able to compensate the loss introduced by the modulators and coaxial cables and hence improve the bandwidth to 5.8GHz. We also measured the eye opening before and after using SEPD. The result shown in Fig. 10(c) clearly proves the ability of SEPD to equalize the data and improve the eye opening.

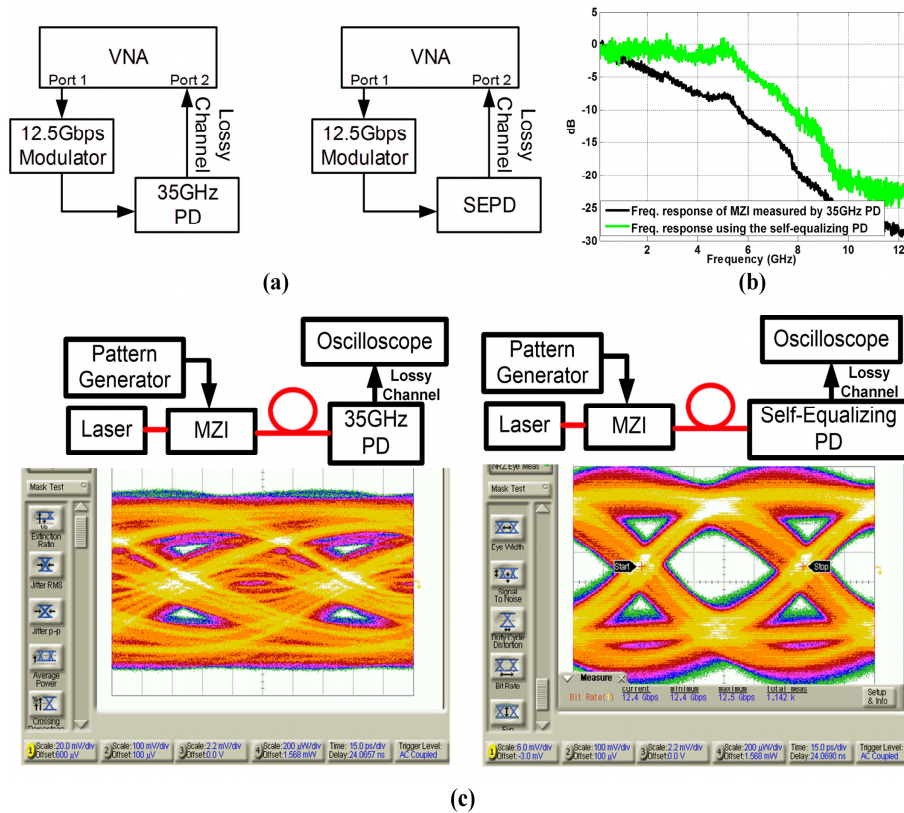


Fig. 10. Measurement results showing bandwidth enhancement in a bandwidth limited optical link. (a) Measurement setup for measuring the electro-optical bandwidth using a 35GHz PD and SEPD. (b) Comparison of the two measured frequency responses showing 7dB of enhancement. (c) Comparison of 12.5Gbps eye-diagrams of the received data without and with SEPD.

Figure 11 shows the adjustability of frequency response in the adjustable self-equalizing photo detector. Depending on the values and sign of the coefficients a wide variety of

frequency responses can be realized with the architectures. As a result, a wide variety of data channels can be equalized.

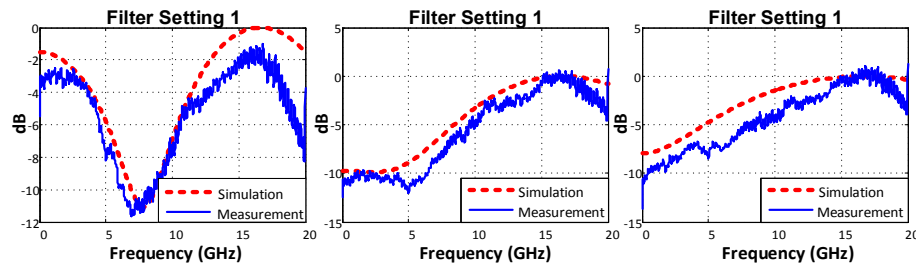


Fig. 11. Demonstration of frequency response adjustment capability in ASEPD.

The ability of the equalizer to improve the eye-opening of the received signal is shown in Fig. 12(a). In the left image, we are showing the 25Gbps received eye diagram, detected with a 35GHz photodiode. The eye is closed because a 12.5Gbps modulator is used which doesn't have sufficient bandwidth for 25Gbps operation. Substituting the commercial photodiode with the proposed ASEPD results in an open eye diagram, showing that a data-rate enhancement factor of two is possible.

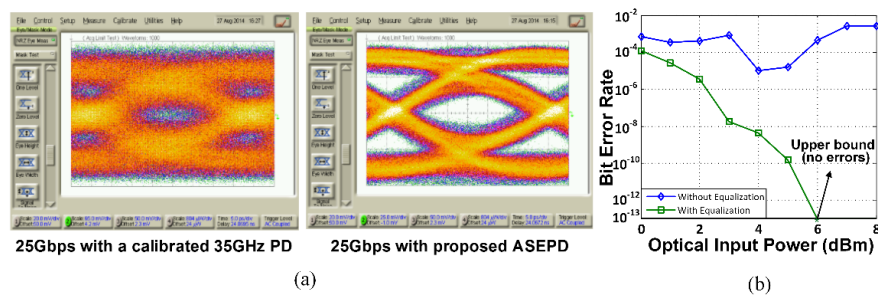


Fig. 12. (a) Demonstration of eye opening capability of the ASEPD at 25Gbps. (b) Demonstration of improvement in receiver sensitivity before and after utilization of ASEPD for a bandwidth limited channel at 12.5Gbps.

Figure 12(b) shows the improvement in the sensitivity of the receiver in a bandwidth limited channel when ASEPD is used in a 12.5Gbps link with PRBS 7 pattern generator. Without equalization and using one of the on-chip photodiodes, the best bit-error-rate (BER) achieved is 10^{-5} . Using the ASEPD, the sensitivity of the receiver improves. No errors were detected in one hour of measurement which demonstrates BER better than 10^{-13} .

5. Conclusion

In this paper we demonstrated an electro-optical approach to equalize and improve the receiving optical signal in an optical communication link and perform the electro-optical conversion in one device. The proposed approach overcomes some of the shortcoming that are inherent to fully electrical or fully optical equalizers. Two working prototypes of the concept in which one has fixed tap coefficients and consumes no power and the other has adjustable tap coefficients and is suited for a wide variety of optical links were demonstrated. It was shown that both prototypes are capable of equalizing the received eye-diagram and allow for higher data rate transmission than otherwise would have been possible.

Acknowledgments

The authors would like to thank Dr. Tom Baehr-Jones and Dr. Michael Hochberg for chip fabrication through OpSIS and Andy Zhou for the help in measurement.